Metallomics

PAPER

View Article Online
View Journal | View Issue

Cite this: *Metallomics*, 2014, 6, 356

The role of glutathione in mercury tolerance resembles its function under cadmium stress in *Arabidopsis*†

Juan Sobrino-Plata,[ab] Sandra Carrasco-Gil,[ac] Javier Abadía,[c] Carolina Escobar,[b] Ana Álvarez-Fernández[c] and Luis E. Hernández*[a]

Received 5th November 2013,
Accepted 23rd December 2013

DOI: 10.1039/c3mt00329a

www.rsc.org/metallomics

Recent research efforts have highlighted the importance of glutathione (GSH) as a key antioxidant metabolite for metal tolerance in plants. Little is known about the mechanisms involved in stress due to mercury (Hg), one of the most hazardous metals to the environment and human health. To understand the implication of GSH metabolism for Hg tolerance, we used two γ-glutamylcysteine synthetase (γECS) *Arabidopsis thaliana* allele mutants (*rax1-1* and *cad2-1*) and a phytochelatin synthase (PCS) mutant (*cad1-3*). The leaves of these mutants and of wild type (Col-0) were infiltrated with a solution containing Cd or Hg (0, 3 and 30 μM) and incubated for 24 and 48 h. The formation of phytochelatins (PCs) in the leaf extracts was followed by two different HPLC-based methods and occurred in Col-0, *cad2-1* and *rax1-1* plants exposed to Cd, whereas in the Hg treatments, PCs accumulated mainly in Col-0 and *rax1-1*, where Hg–PC complexes were also detected. ASA and GSH/GSSG levels increased under moderate metal stress conditions, accompanied by increased GSH reductase (GR) activity and expression. However, higher metal doses led to a decrease in the analysed parameters, and stronger toxic effects appeared with 30 μM Hg. The GSH concentration was significantly higher in *rax1-1* (70% of Col-0) than in *cad2-1* (40% of Col-0). The leaves of *rax1-1* were less sensitive than *cad2-1*, in accordance with the greater expression of γECS in *rax1-1*. Our results underline the existence of a minimal GSH concentration threshold needed to minimise the toxic effects exerted by Hg.

Introduction

Important advances have been made in recent years in understanding the mechanisms of plant tolerance to hazardous metals. Among these toxic elements, mercury (Hg) requires major attention due to its particular physicochemical properties, which render it an extremely toxic metal for the environment and for humans. In fact, severe restrictions in its industrial application and trading have been imposed in recent years to prevent environmental and health risks.[1] This metal can be found in most ecosystems in three different oxidation forms: metallic (Hg^0), monovalent (Hg_2^{2+}) or divalent (Hg^{2+}), the last form being the most abundant in well-aerated environments. Mercury is found frequently in minerals associated with Cl^-, OH^- and reduced sulphur (*i.e.*, cinnabar) but can also bind directly to carbon, forming organomercurials, such as methylmercury (CH_3Hg; MeHg) or dimethylmercury (CH_3HgCH_3), which are the most toxic Hg species in nature. MeHg is mainly the result of microbial activity in the environment and can bioconcentrate and biomagnify in the food chain, as occurred in the Minamata (Japan) poisoning incident.[2]

Plants are able to absorb and accumulate Hg from polluted soils mainly as Hg^{2+}, which may constitute the main entrance of Hg into terrestrial ecosystems. The accumulation of Hg causes several toxic symptoms, such as the inhibition of plant growth and the induction of oxidative stress.[3] The strong affinity of Hg^{2+} for sulfhydryl groups is one of the mechanisms that provokes severe alterations of protein structure and function (structural proteins in membranes and the inhibition of several enzymatic processes) in a similar manner as cadmium (Cd) and copper (Cu) exert when accumulated at phytotoxic concentrations.[4] However, Hg provokes stronger harmful effects than does Cd when plants are treated with similar doses, causing, in particular, a more rapid induction of oxidative stress and cell death.[5]

Many aerobic processes in plant metabolism generate reactive oxygen species (ROS), which are mostly partially reduced

[a] *Laboratory of Plant Physiology, Department of Biology, Universidad Autónoma de Madrid, Cantoblanco, 28049 Madrid, Spain. E-mail: luise.hernandez@uam.es*
[b] *Department of Environmental Sciences, Universidad de Castilla la Mancha, Campus Fábrica de Armas, 45070 Toledo, Spain*
[c] *Department of Plant Nutrition, Estación Experimental de Aula Dei (CSIC), Av. Montañana 1005, E-50080, Zaragoza, Spain*

† Electronic supplementary information (ESI) available. See DOI: 10.1039/c3mt00329a

intermediates of oxygen, such as hydrogen peroxide (H_2O_2) or superoxide anion radicals ($O_2^{\bullet -}$). Some of these molecules play important roles in stress signalling and perception, cell cycle regulation, photosynthesis and cell wall lignification.[6] However, under biotic or abiotic stresses, the production of ROS is enhanced, and oxidation reactions occur with different macromolecules,[7] leading to several degrees of cellular damage. In this respect, the relevant role of glutathione (GSH) in counteracting the phytotoxic effects of diverse toxic metals is highlighted.[8,9] Glutathione is a tripeptide that is synthesised from glycine (Gly), glutamate (Glu) and cysteine (Cys), amino acid that harbours a thiol group that provides the chemical properties of this antioxidant metabolite.[10] In addition to its cellular redox homeostasis and organic sulphur storage roles, many important functions of GSH have recently been discovered, from the detoxification of xenobiotics to cellular signalling and development.[11] The biosynthesis of GSH has been widely studied.[12,13] This process is carried out in two ATP-dependent enzymatic steps. First, gamma-glutamylcysteine synthetase (γECS) binds Cys and Glu to form the intermediate γ-glutamylcysteine (γEC); second, GSH is formed by glutathione synthetase (GS) by the binding of glycine (Gly) to γEC. This process is highly compartmentalised, as γECS is located entirely in the plastids, whereas GS occurs mainly, but not exclusively, in the cytosol.[14]

To control the levels of ROS, plant cells possess an antioxidant system composed of enzymes and metabolites in which the ascorbate (ASA)–glutathione (GSH) cycle plays a central role.[15] In this cycle, excess ROS are removed by the reduction of H_2O_2 to H_2O, consuming ascorbate *via* ascorbate peroxidase (APX) and forming monodehydroascorbate (MDHA), which ultimately is converted to dehydroascorbate (DHA) in a rapid non-enzymatic reaction.[7] The enzyme dehydroascorbate reductase consumes GSH to regenerate ascorbate, accumulating oxidised glutathione (GSSG).[15] The cellular pool of reduced GSH is maintained, in turn, by glutathione reductase (GR), an enzyme that consumes NADPH. GR is a homodimer protein located in different organelles, including chloroplasts and mitochondria, or in the cytosol; however, in photosynthetic cells, up to 80% of GR activity is associated with chloroplasts. GR is considered a relevant component of the antioxidant machinery, maintaining the correct GSH/GSSG ratio, which is fundamental for the redox homeostasis of the cell.[16]

An important mechanism of Hg detoxification is based on its high affinity for sulfhydryl groups through the formation of Hg–phytochelatin (Hg–PCs) complexes.[17] Phytochelatins (PCs) are synthesised by the enzyme phytochelatin synthase (PCS), which condenses γEC molecules into GSH (($(\gamma GluCys)_n Gly$), where n is between 2 and 11). It is thought that PCs are transported into the vacuole while bound to the metal during the final step of metal detoxification.[18]

Glutathione may play a dual protective role in plant toxic metal tolerance, both as an antioxidant and as a precursor of PCs; this hypothesis is based on the drastic changes observed in its metabolism, particularly under Cd stress.[9] However, little is known about the function of GSH in Hg homeostasis, despite the recent findings regarding the protection acquired by the chelation of Hg with PCs.[17] Therefore, we studied the behaviour of two γECS mutant alleles of *Arabidopsis thaliana* that accumulate lower GSH levels than does the wild type genotype (Columbia 0; Col-0): *cadmium-sensitive 2-1* (*cad2-1*) and *regulator of APX2 1-1* (*rax1-1*), which contain 30% and 45% of the GSH found in Col-0 plants, respectively.[19,20] We also evaluated the responses of a PC synthesis-defective mutant, *cadmium-sensitive 1-3* (*cad1-3*), which expresses a non-functional PCS.[21] We infiltrated the leaves of these *Arabidopsis* genotypes with different concentrations of Hg and Cd (a potent inducer of PC synthesis) to characterise in detail the short-term adjustments in the GSH metabolism induced by these toxic metals.

Experimental

Plant material, growth conditions and treatments

Arabidopsis thaliana seeds of wild type (Col-0), *cad2-1*, *rax1-1* and *cad1-3* genotypes were surface-sterilised by agitation in a 15% (v/v) NaOCl solution for 10 min, followed by several rinses in distilled sterile water. The seeds were germinated in square Petri dishes in solid Murashige–Skoog nutrient medium (0.6% Phyto-agar, Duchefa Biochemie B.V., Haarlem, The Netherlands) supplemented with 2% sucrose for 5 days under a long-day light regime at 25 °C. After this period, the seedlings were grown in a perlite : peat (1 : 3) mixture for 1 month under a short-day light regime. The leaves were cut into 1 cm diameter disks, placed into 15 mL glass tubes, sealed with silicone septum stoppers, and infiltrated under vacuum with deionised water (control), $CdCl_2$ or $HgCl_2$ solutions (3 or 30 μM). The disks were incubated at 20 °C with continuous illumination for 24 and 48 hours (Fig. S1, ESI†). Before storing, the disks were washed with 10 mM Na_2EDTA and deionised water to remove any adsorbed superficial heavy metals, snap-frozen in liquid nitrogen and stored at −80 °C until analysis.

Chemicals and antibodies

All of the products were of analytical grade (≥99.0%). All of the eluents, extraction buffers, and standard solutions were prepared with analytical-grade type I water (Milli-Q Synthesis, Millipore, Bedford, MA, USA). Acetonitrile HPLC-gradient grade was purchased from Scharlab S.L. (Barcelona, Spain); formic acid was purchased from Fluka (Sigma-Aldrich, St. Louis, MO, USA); GSH, GSSG, ASA, *N*-acetylcysteine, Protease Inhibitor Cocktail P2714 and *Saccharomyces cerevisiae* GR were purchased from Sigma-Aldrich (St. Louis, MO, USA); and labelled GSH ([glycine 1,2-^{13}C,^{15}N]GSH) and ASA ([1-^{13}C]ASA) were obtained from Cambridge Isotope Laboratories (Andover, MA, USA). PC_2, PC_3 and PC_4 were purchased from Peptide 2.0 (Chantilly, VA, USA). A LumiSensor Chemiluminescent HRP Substrate Kit (L00221V60) and the Goat Anti-Rabbit IgG Antibody (H&L) conjugated with horseradish peroxidase (α-IgG; A00160) were acquired from GenScript (Piscataway, NJ, USA). Rabbit polyclonal antibodies anti-GR (α-GR; AS06181) and anti-γECS (α-γECS; AS06186) were purchased from Agrisera (Vännäs, Sweden).

Cadmium and mercury analyses by ICP-MS

Leaf disks were dried at 50 °C for 72 h, homogenised with a mortar and pestle, and acid-digested under pressure in

chromatographic vials (4 mL capacity) sealed with polytetrafluoroethylene stoppers. A 100 mg aliquot of the dried powder was mixed with a 1 mL digestion reagent (HNO_3 : H_2O_2 : H_2O, 0.6 : 0.4 : 1 v : v) and autoclaved (Presoclave-75 Selecta, Barcelona, Spain) at 120 °C and 1.5 atm for 30 min.[5] The digests were filtered through a PVDF filter and diluted in milli-RO water to 5 mL. The Cd and Hg concentrations were determined using ICP-MS NexION 300 (Perkin-Elmer Sciex, San Jose, CA, USA).

Analysis of biothiols by HPLC/UV-VIS and post-column derivatisation

Biothiols were analysed by high performance liquid chromatography (HPLC) using an Agilent 1200 HPLC system (Santa Clara, CA, USA) following the procedure described by Ortega-Villasante *et al.*[22] A 100 mg aliquot of frozen intact leaf tissue was homogenised in a solution of 0.125 N HCl, which contained 0.25 mM *N*-acetylcysteine as an internal standard for quantification.[21] The homogenate obtained was centrifuged at 14 000 × *g* for 15 min at 4 °C. The extracts (100 μL) were injected into a Mediterranea SEA18 column (5 μm, 250 × 4.6 mm; Teknokroma, SantCugat del Vallès, Spain) and eluted with a gradient mobile phase built with 98 : 2 H_2O : acetonitrile (v/v) in 0.01% TFA (solvent A) and 2 : 98 dH_2O : acetonitrile (v/v) in 0.01% TFA (solvent B). The gradient program, regarding the % solvent B, was as follows: 2 min, 0%; 25 min, 25%; 26 min, 50%; 30 min, 50%; 35 min, 0%, 45 min, 0%. Detection was achieved after post-column derivatisation with Ellman's reagent [1.8 mM 5,5-dithiobis(2-nitrobenzoic) acid in 300 mM K-phosphate, 15 mM EDTA at pH 7.0] in a thermostatic 1.8 mL reactor at 38 °C as described by Rauser.[23] Biothiols were identified by the derivative compound 5-mercapto-2-nitrobenzoate (maximum absorption at 412 nm) using commercially available standards (Cys, GSH, PC_2, PC_3, and PC_4).

Analysis of GSH, GSSG, ASA and complexes of biothiols with mercury by HPLC/ESI-MS(TOF)

Isotopically labelled GSH (GSH*) and ASA (ASA*) were used as internal standards and added to the leaf disks immediately before the extraction as described by Rellán-Álvarez *et al.*[24] The final concentration of GSH* and ASA* in the injected solutions (standards and plant extracts) was 75 and 100 μM, respectively. An HPLC/ESI-MS(TOF) analysis was carried out using an Alliance 2795 HPLC system (Waters, Milford, MA, USA) coupled to a time-of-flight mass spectrometer (micrOTOF, Bruker Daltonics, Bremen, Germany) equipped with an electro-spray (ESI) source following the method described by Rellán-Álvarez *et al.*[24] with minor modifications (Method S1, ESI†). The mass axis was calibrated externally using Li-formate adducts (10 mM LiOH, 0.2% (v/v) formic acid and 50% (v/v) 2-propanol). The HPLC/ESI-TOF MS system was controlled using the software packages micrOTOF Control v.2.2 and HyStar v.3.2 (Bruker Daltonics). The data were processed using Data Analysis v.4.0 (Bruker Daltonics). Ion chromatograms were always extracted with a precision of ±0.05 *m*/*z* units. Mercury complexes and PC ligands were identified as described by Carrasco-Gil *et al.*[17]

Glutathione reductase activity *in gel*

The glutathione reductase activity was determined *in gel* after separating the protein extracts by non-denaturing electrophoresis in 10% polyacrylamide gels. Five hundred milligrams of intact frozen material were homogenised in 1 mL extraction solution (30 mM MOPS at pH 7.5, 5 mM Na_2-EDTA, 10 mM DTT, 10 mM ascorbic acid, and 0.6% PVPP supplemented with 100 μM PMSF and Protease Inhibitor Cocktail) and centrifuged at 14 000 × *g* and 4 °C for 15 min. The protein concentration was determined using the Protein Assay Reagent (Bio-Rad, Hercules, CA, USA), and the final protein loading was adjusted by denaturing gel electrophoresis and Coomassie-blue staining.[25] The protein loading for GR analysis was 15 μg, and the GR activity was revealed as described by Sobrino-Plata *et al.*[26]

Western blot and immunodetection

Immunodetection was performed by western blot after the denaturing gel electrophoresis.[25] Once the proteins were separated (10 μg total protein), they were blotted onto a nitrocellulose membrane (BioTrace® NT Pall Corporation, East Hills, NY, USA) using a semi-dry procedure (Trans Blot® SD Semi-Dry Electrophoretic Transfer Cell; Bio-Rad). The gel slabs were briefly incubated in transfer buffer (48 mM Tris-HCl, 39 mM glycine, 1.3 mM SDS, and 20% methanol at pH 8.3) and then electroblotted for 1 h. The membrane was blocked with 1% BSA in Tris-buffer-saline (TBS) and incubated overnight at 4 °C with the primary antibodies (α-GR, dil. 1/5000; α-γECS, dil. 1/2500). After several washes with TBS, the membrane was incubated with the secondary antibody diluted 1/10 000 for 1 h. The proteins were detected by incubating for 2 minutes with the LumiSensor Chemiluminescent HRP Substrate Kit, and images were taken with the ChemiDoc™ XRS+ System (Bio-Rad).

Statistics

Statistical analysis was performed using the software package SPSS for Windows (v. 19.0) using an ANOVA with Tukey's test. The results presented are means of at least four replicates ± standard deviation and are considered significantly different at $p < 0.05$.

Results

Cadmium and mercury concentrations

The metal concentration in Col-0 leaf disks increased in a dose-dependent manner. The Cd concentration in the disks increased with time; an incubation of 48 h produced an accumulation of 4 times the concentration found at 24 h (Fig. 1). However, the Hg concentration was similar after 24 and 48 h of treatment, indicating that the Hg accumulation was saturated (Fig. 1). There were no statistically significant differences of the metal concentration between the leaves of Col-0 and γECS or PCS mutants (data not shown).

Biothiol concentration

The biothiol analysis of *Arabidopsis* leaf disks by conventional HPLC revealed that Cys accumulated similarly in most

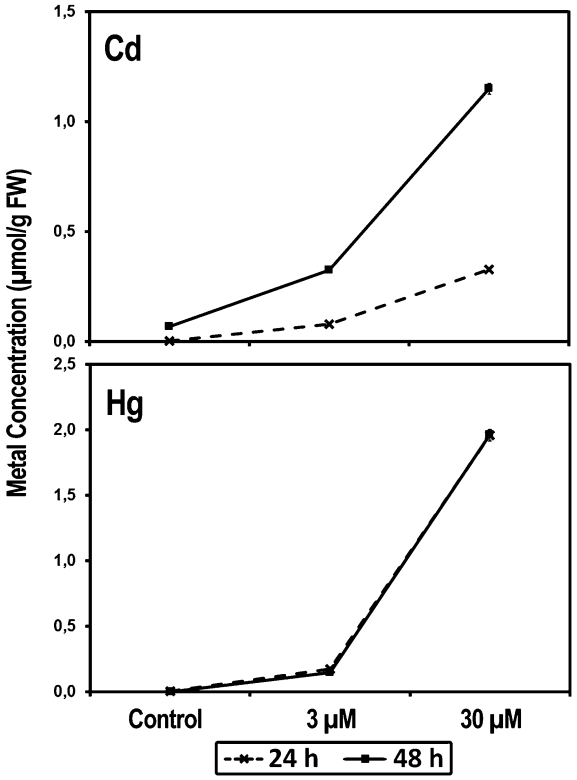

Fig. 1 Concentrations of Cd and Hg (µmol g^{-1} FW) in disks of Col-0 *Arabidopsis thaliana* leaves treated with 0, 3, or 30 µM Cd or Hg incubated for 24 and 48 hours. The standard error bars were smaller than the symbols.

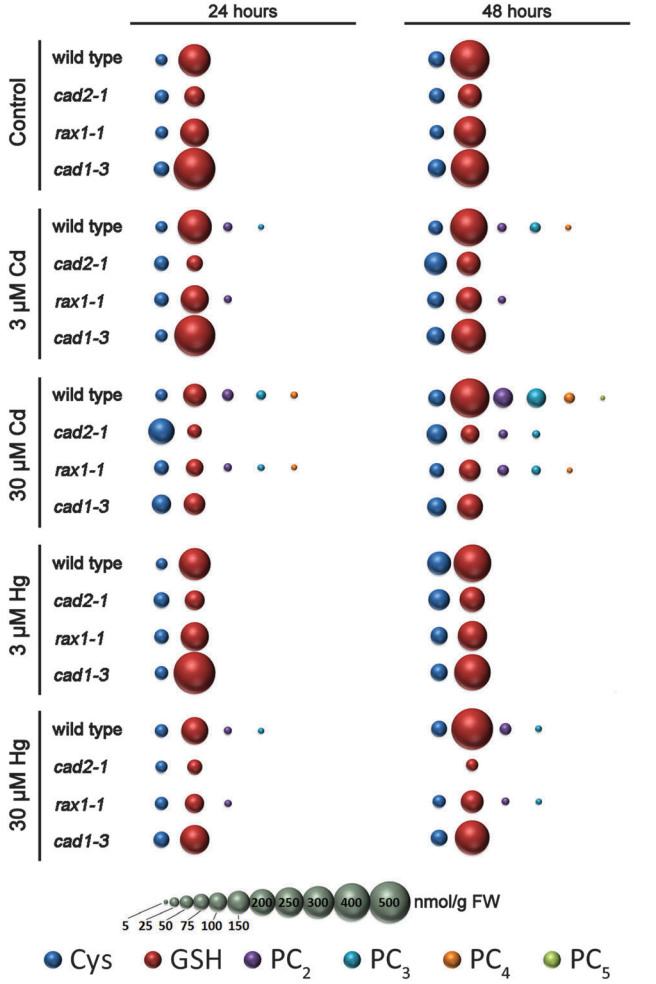

Fig. 2 Biothiol concentration (nmol g^{-1} FW) of leaf disks from Col-0, *cad2-1*, *rax1-1* and *cad1-3 Arabidopsis thaliana* leaves infiltrated with 0, 3, or 30 µM Cd or Hg for 24 and 48 h. Different biothiols are represented by spheres with different colours, and the concentrations correspond to different diameters. The concentration-to-diameter scale is shown by the grey spheres at the bottom. For statistics, please see Table S1 (ESI†).

genotypes but increased remarkably in *cad2-1* exposed to 30 µM Cd in both incubation periods (Fig. 2; Table S1, ESI†). There was also a significant increase in the Cys concentration in Col-0 and *cad2-1* treated with 3 µM Hg for 48 h, while under 30 µM Hg, the Cys concentration decreased in all of the γECS mutants, with a strong diminution in *cad2-1*, where levels were below the detection limit (Fig. 2; Table S1, ESI†).

The GSH concentration in the γECS mutants under control conditions was lower than in Col-0 by 40% (*cad2-1*) and 70% (*rax1-1*). The PC-defective mutant *cad1-3* showed higher GSH levels than did Col-0, except when treated with 30 µM Cd and Hg for 48 h (Fig. 2). Exposure to Cd in the γECS mutants caused a clear decrease in the GSH concentration in a dose-dependent manner that was more marked in *rax1-1*. Interestingly, this effect was accompanied by the accumulation of PCs but at a smaller degree than that observed in Col-0 (Fig. 2). No changes in the GSH levels were observed with the lowest concentration of Hg in any of the genotypes at both incubation times. However, the concentration of GSH in the γECS mutants decreased by half that of the control levels with 30 µM Hg; this decrease was less pronounced in Col-0 (Fig. 2 and Table S1, ESI†).

Cadmium was a stronger inducer of PC synthesis than was Hg: the PC concentration in Col-0 leaves with 30 µM Cd was double that in those with 30 µM Hg after the 24 h incubation. It was possible to detect PC_2 ($(\gamma Glu\text{-}Cys)_2$-Gly), PC_3 ($(\gamma Glu\text{-}Cys)_3$-Gly) and PC_4 ($(\gamma Glu\text{-}Cys)_4$-Gly). Larger differences in this response were found when the treatment was prolonged to 48 h, as it was even possible to detect some PCs (PC_2 and PC_3) in the *cad2-1* leaves despite its poor GSH level (Fig. 2 and Table S1, ESI†). Col-0 and *rax1-1* displayed a similar behaviour regarding the formation of PCs, although the occurrence of PCs in the γECS mutant (all of the PCs except for PC_5 ($(\gamma Glu\text{-}Cys)_5$-Gly)) was lower in terms of molecular weight and concentration, as observed when exposed to 30 µM Cd. No PC accumulation was observed in the *cad1-3* leaves, confirming the PCS knock-out mutation (Fig. 2). Mercury induced the accumulation of PC_2 and PC_3 only in Col-0 and *rax1-1*, being lower in the latter (Fig. 2 and Table S1, ESI†).

GSH, GSSG and ASA concentrations

The ASA, GSH and GSSG concentrations were determined in disks of *A. thaliana* leaves treated with Cd and Hg by HPLC/ESI-MS(TOF) using isotopically labelled ASA and GSH as internal standards. In agreement with the analysis performed with conventional HPLC, the GSH levels in the γECS mutants were significantly

lower than those in Col-0 and *cad1-3*. The GSH concentration increased in Col-0 and *rax1-1*, but particularly in *cad1-3* when exposed to 3 μM Cd or Hg for 24 h (Fig. 3A). In parallel, the ASA and GSSG concentrations increased even more in leaves treated with 3 μM Cd, which led to a higher GSSG-to-total GSH ratio. However, the GSH concentration returned to control values when the leaf disks were treated with 30 μM Cd or Hg. In this case, the concentrations of ASA and GSSG decreased in general compared with those of leaves treated with the lowest metal dose, following a typical hormetic response. Therefore, under

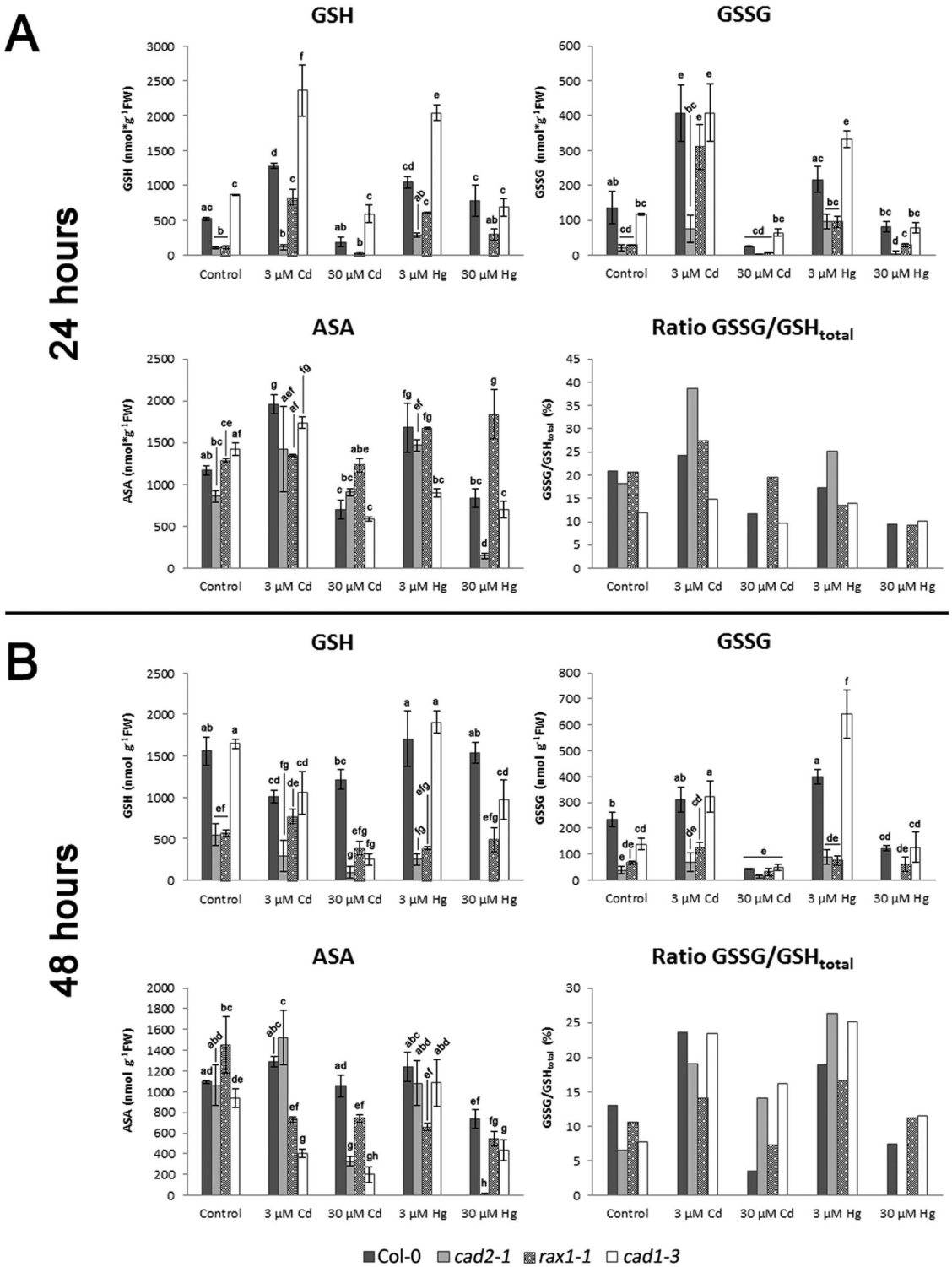

Fig. 3 Concentrations of GSH, GSSG and ASA (nmol g^{-1} FW) and the GSSG-to-total GSH ratio (%) in the disks of Col-0, *cad2-1*, *rax1-1* and *cad1-3* *Arabidopsis thaliana* leaves infiltrated with 0, 3, or 30 μM Cd or Hg incubated for 24 (A) and 48 h (B).

30 μM Cd or Hg, the GSSG-to-total GSH ratio was lower than in the control samples (Fig. 3A). A different pattern was observed in leaves treated for 48 h: the GSH concentration decreased in a dose-dependent manner. The highest levels of GSSG were found in leaves exposed to 3 μM Cd or Hg, values that were particularly high in *cad1-3* (Fig. 3B). Conversely, the GSSG concentration of leaves incubated with 30 μM Cd or Hg decreased sharply to values below those of the controls. The ASA concentration remained at a level similar to that of the controls, but dropped when exposed to 30 μM Cd or Hg (Fig. 3B).

Detection of free PCs and Hg–PC complexes

Ion chromatograms of free ligands and Hg–thiol complexes were extracted at the exact mass-to-charge ratio (*m*/*z*) corresponding to $[M–H]^-$ ions from the HPLC/ESI-MS(TOF) analyses. The Hg–PC complexes were identified based on the characteristic natural Hg isotopic signature: (^{196}Hg, ^{198}Hg, ^{199}Hg, ^{200}Hg, ^{202}Hg, ^{204}Hg) according to Carrasco-Gil *et al.*,[17] and the chromatograms were extracted always with the *m*/*z* corresponding to the most abundant stable isotope of Hg (^{202}Hg). Several examples of chromatograms and zoomed-MS spectra showing signals matching with free PCs and Hg-linked ligands occurring in the leaf disks of Col-0 (Fig. 4A) and *rax1-1* (Fig. 4B) incubated with 30 μM Hg for 48 h can be found in Fig. 4. The ligands (PC_2, Fig. 4C) and Hg–PC complexes (Hg–PC_2 and Hg–PC_3, Fig. 4D and H) were identified by the comparison of the analytical and theoretical spectrum, predicted with the micrOTOF Data Analysis Software (see insets in the different panels of Fig. 4). In addition, several PCs were oxidised, having intramolecular disulphide bonds (for example, oxidised PC_3, Fig. 4G), leading to an *m*/*z* loss of 2 Da compared to the *m*/*z* of its reduced form.

Biothiol complexes with Cd were not detected in the HPLC/ESI-MS(TOF) analysis due to the strong acidic conditions used during the extraction and the chromatographic separation that could lead to the total dissociation of these complexes. However, we could identify in these samples several biothiol ligands (Table 1), some of which could not be detected by conventional HPLC analysis, such as oxidised PC_2, PC_3, PC_4 or PC_5. No PC occurrence was detected in *cad1-3*. The Col-0 leaves accumulated a wide array of ligands, being capable of synthesising even PC_6 ($(\gamma$-Glu-Cys$)_6$-Gly) after 48 h of treatment with 30 μM Cd. The leaves of *rax1-1* were also able to accumulate a similar variety of PCs as were those of Col-0, but with slightly less diversity. As expected, *cad2-1* accumulated a less varied population of PC ligands, which augmented also with time of exposure to Cd.

Both of the Hg treatments (3 and 30 μM) induced the formation of PC_2 and PC_3 in Col-0 and *rax1-1* leaves treated for 48 h. When the leaves were incubated with 3 μM Hg for 24 h, we could only detect PC_2, a ligand that was also surprisingly found in *cad2-1* just above the background spectral noise (Table 1). Complexes of PC_2 and PC_3 with Hg were only found in Col-0 and *rax1-1* samples treated with 30 μM Hg for 24 or 48 h. Although we were not able to quantify the Hg–PC

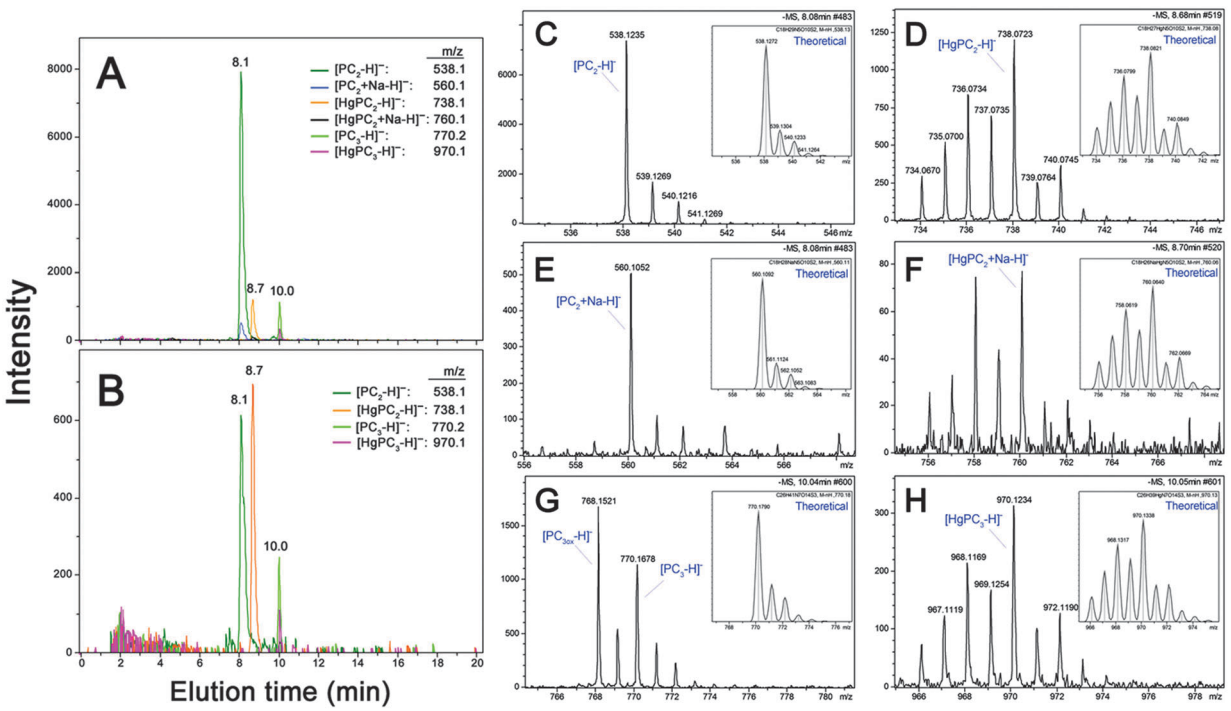

Fig. 4 HPLC/ESI-MS(TOF) analysis of biothiol ligands and Hg–biothiol complexes in Col-0 (A) and *rax1-1* (B) leaves infiltrated with 30 μM Hg and incubated for 48 hours. The peaks corresponding to different biothiol ligands and Hg–biothiol complexes are shown. Examples of zoomed-MS spectra obtained from the analyses of Col-0 disks that show the experimental isotopic signature corresponding to PC_2 (C), Hg–PC_2 (D), PC_2 + Na (E), Hg–PC_2 + Na (F), PC_3 (G), and Hg–PC_3 (H). Theoretical isotopic signatures corresponding to the identified molecular ions are shown in the insets.

Table 1 Ligands and Hg–PC complexes detected in negative mode by the HPLC/ESI-TOF (MS) of Col-0, *cad2-1* and *rax1 Arabidopsis thaliana* leaves treated with 0, 3 or 30 μM Cd or Hg for 24 and 48 h. The identification of the detected ions is indicated by their mass-to-charge ratio (*m*/*z*) and chromatographic retention times (t_R; in minutes). Different colours were chosen for each genotype: purple, Col-0; green, *cad2-1*; red, *rax1-1*. Pale and dark tones indicate, respectively, the presence of ligands in the 3 or 30 μM metal treatments. The data were obtained from 3 independent biological replicates

Molecular ion	*m*/*z*	t_R	24 h						48 h					
			Col-0		*cad2-1*		*rax1-1*		Col-0		*cad2-1*		*rax1-1*	
Cadmium (μM)			3	30	3	30	3	30	3	30	3	30	3	30
$[PC_2–H]^-$	538.1	8.0												
$[PC_{2ox}–H]^-$	536.1	8.0												
$[PC_3–H]^-$	770.2	10.0												
$[PC_{3ox}–H]^-$	768.2	10.0												
$[PC_4–H]^-$	1002.2	10.1												
$[PC_{4ox}–H]^-$	1000.2	10.1												
$[PC_4–2H]^{2-}$	500.6	10.1												
$[PC_{4ox}–2H]^{2-}$	498.6	10.1												
$[PC_5–2H]^{2-}$	616.6	10.2												
$[PC_{5ox}–2H]^{2-}$	614.6	10.2												
$[PC_6–2H]^{2-}$	732.7	10.2												
Mercury (μM)														
$[PC_2–H]^-$	538.1	8.0												
$[PC_{2ox}–H]^-$	536.1	8.0												
$[PC_3–H]^-$	770.2	10.0												
$[PC_{3ox}–H]^-$	768.2	10.0												
$[HgPC_2–H]^-$	738.1	8.7												
$[HgPC_3–H]^-$	970.1	10.1												

complexes, the signal intensity corresponding to these Hg complexes in *rax1-1* was normally 10-fold lower than that in Col-0.

Characterisation of γECS and GR under metal stress

To complete our study, we evaluated the state of two important enzymes in GSH metabolism: γECS, the first enzyme of the GSH biosynthesis pathway, and GR, which is important in maintaining the pool of reduced GSH in the cells. Regarding γECS, *rax1-1* showed in general a higher accumulation than did the other genotypes. γECS was remarkably expressed in *rax1-1* compared to its expression in Col-0, *cad2-1* and *cad1-3* in all of the leaf disks treated with Cd (Fig. 5), except for those treated with 3 μM Cd for 48 h, which had exhibited over-expression of γECS in Col-0 and *cad1-3* (Fig. 5f).

The Hg treatments also led to the over-expression of γECS in leaves from *rax1-1* when Hg was applied at 3 μM for 48 h and 30 μM for 24 h (Fig. 6b and f). However, *cad2-1* showed a different γECS expression pattern than that of *rax1-1* without any apparent changes compared to that of Col-0 in all of the treatments and exposure times, but showed a strong down-regulation in disks incubated with 30 μM Hg for 48 h (Fig. 6f). It should also be noted that the proteins extracted from *cad2-1* treated for 48 h with 30 μM Hg were partially denatured (Fig. 6f).

The activity of GR increased mainly in a dose-dependent manner in leaf disks treated with Cd for either 24 or 48 h, independent of the genotype (Fig. 5d and h). The immunodetection using α-GR revealed a general over-expression in all of the genotypes in leaves treated with Cd, an effect that was more marked after 48 h of exposure (Fig. 5c and g). However, the Hg treatments led to different effects on the GR activity that were dependent on the dose and time of exposure (Fig. 6). All of the genotypes showed a remarkable increase in GR activity after 24 h of treatment with 3 μM Hg. In addition, the *rax1-1* and *cad1-3* GR activities also increased under 30 μM Hg after 24 h but were inhibited in *cad2-1* (Fig. 6d). A similar behaviour was observed after 48 h of incubation, when the GR activity of all of the genotypes was similar to that of the control samples when exposed to 3 μM Hg, but there was a sharp inhibition of this activity in *cad2-1* leaf disks incubated with 30 μM Hg for 48 h (Fig. 6h). Interestingly, GR was also over-expressed when the leaf disks were challenged with Hg in a dose- and time-dependent manner, with the strongest response occurring in *cad2-1* treated with 30 μM Hg for 48 h (Fig. 6g).

Discussion

Mercury accumulated more than did Cd in the analysed leaf disks, reaching the maximum concentration after 24 h and showing a characteristic saturation pattern, while the Cd concentration increased up to 48 h. Similar results were found in plants treated with identical doses of Hg and Cd, where Hg accumulated to a higher degree in the roots than did Cd.[3,26] The mechanism of Hg uptake in plant cells is not completely understood, but recent research has shown that Hg accumulates preferentially in the cell walls[17,28] and presumably moves

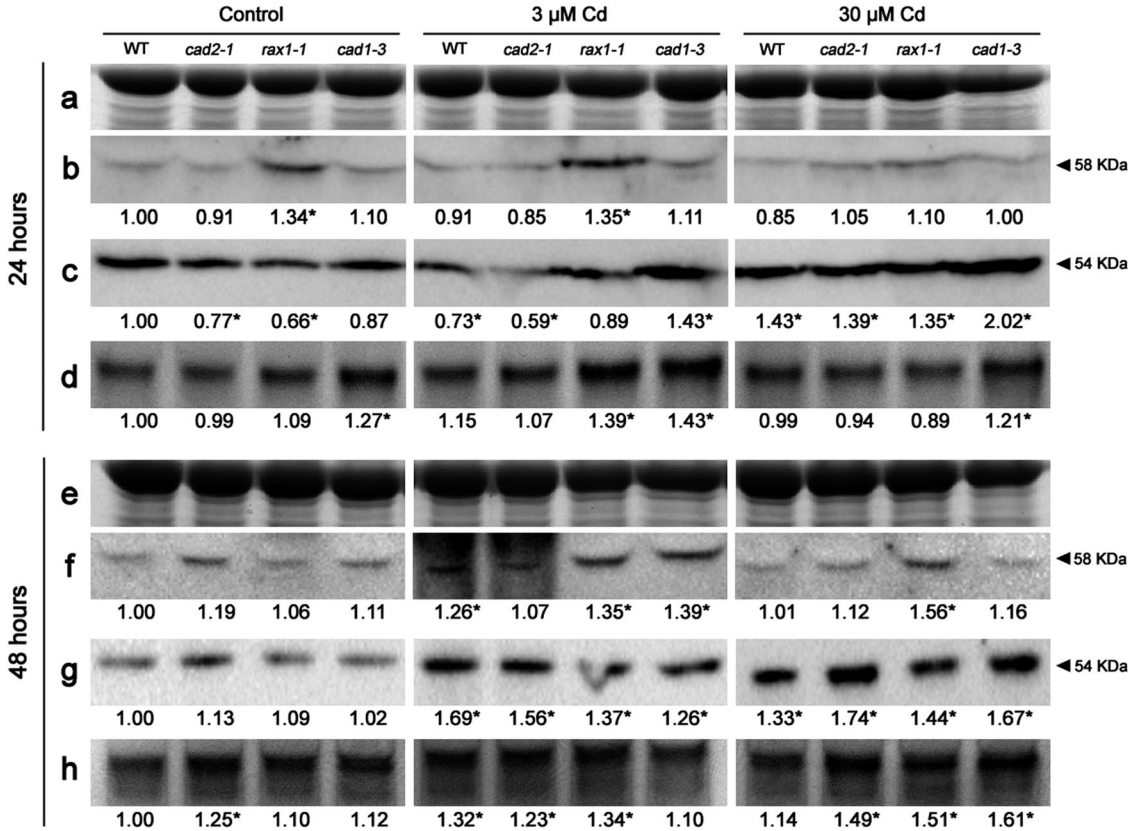

Fig. 5 Immunodetection of γECS (b and f), GR (c and g), and *in gel* GR activity (d and h) in 0, 3, and 30 μM Cd-infiltrated leaves of Col-0, *cad2-1*, *rax1-1* and *cad1-3 Arabidopsis thaliana* incubated for 24 and 48 h. Coomassie Blue (a and e) general staining of proteins to show the equivalent loading of samples. The numbers represent the relative fold-changes against the control, and asterisks mark changes greater than ±20%.

to the aerial part of plants following the apoplastic water flow.[27] Cadmium seems to bind to a lesser degree to cell walls, as this metal has a more balanced distribution between the roots and shoots.[26,29] These differences in mobility and binding capacity to the cell walls might explain at least partially the quick and saturated accumulation of Hg relative to that of Cd in the leaf disks after metal infiltration.

The concentration of GSH in the leaf disks of the γECS mutant alleles *cad2-1* and *rax1-1* was significantly lower than that of Col-0, in agreement with previous results.[19,20] However, subtle differences were found when the GSH concentration was analysed by conventional HPLC (Fig. 2 and Table S1, ESI†) or by HPLC/ESI-MS(TOF) (Fig. 3). This divergence can be explained by the different levels of sensitivity of these detection methods as discussed by Rellán-Álvarez *et al.*[24] when alternative analytical procedures are followed. Both of the γECS mutants displayed a relevant increase in the accumulation of Cys. A similar phenotype was described in *Arabidopsis zin1*, another mutant of γECS that contains less than 20% of the GSH level of Col-0.[30] The exposure of *cad2-1* and *rax1-1* to Cd and Hg resulted in the over-accumulation of Cys, particularly in the *cad2-1* leaf disks (Table S1, ESI†). These responses are in agreement with those observed in *nrc1* mutants, another *Arabidopsis* γECS-defective allele, when treated with 20 μM Cd.[31] It is possible that the accumulation of Cys in the γECS mutants reflects an alteration in the sulphur assimilation pathway, in which several enzymatic steps could be up-regulated to increase the concentration of Cys required to augment the GSH concentration under stress.[32] Interestingly, the amplitude of the response may depend on the GSH concentration, as the increase in the Cys concentration was milder in *rax1-1* than in *cad2-1*, mutants whose GSH concentrations were, respectively, 70% and 40% that of Col-0 (Fig. 2 and Table S1, ESI†). Jobe *et al.*[31] suggested a complex interplay between GSH, Cys or γEC concentrations and the cellular redox homeostasis that affects the overall expression of genes involved in sulphur and GSH metabolisms, such as that occurs with the high-affinity AtSULTR1;2 sulphate transporter.

The alteration in the PC production also led to relevant changes in GSH metabolism, as there was a transient and significant increase in the GSH concentration in *cad1-3* leaf disks after 24 h of incubation, particularly greater when treated with 3 μM Cd or Hg (Fig. 2 and 3 and Table S1, ESI†). These results are in agreement with previous experiments of Cd- and Hg-infiltrated *Arabidopsis* leaves.[17] The function of PCS, an enzyme that is constitutively expressed, in non-metal-stressed plants is still a matter of debate.[33] Phytochelatin synthase is a soluble protein located in the cytosol, and it is thought to intervene in the GSH and GSH-conjugate turnover to form γEC or γEC-conjugates, possibly for Cys recycling.[34] It is possible that in the absence of a functional PCS in *cad1-3* mutants, lower

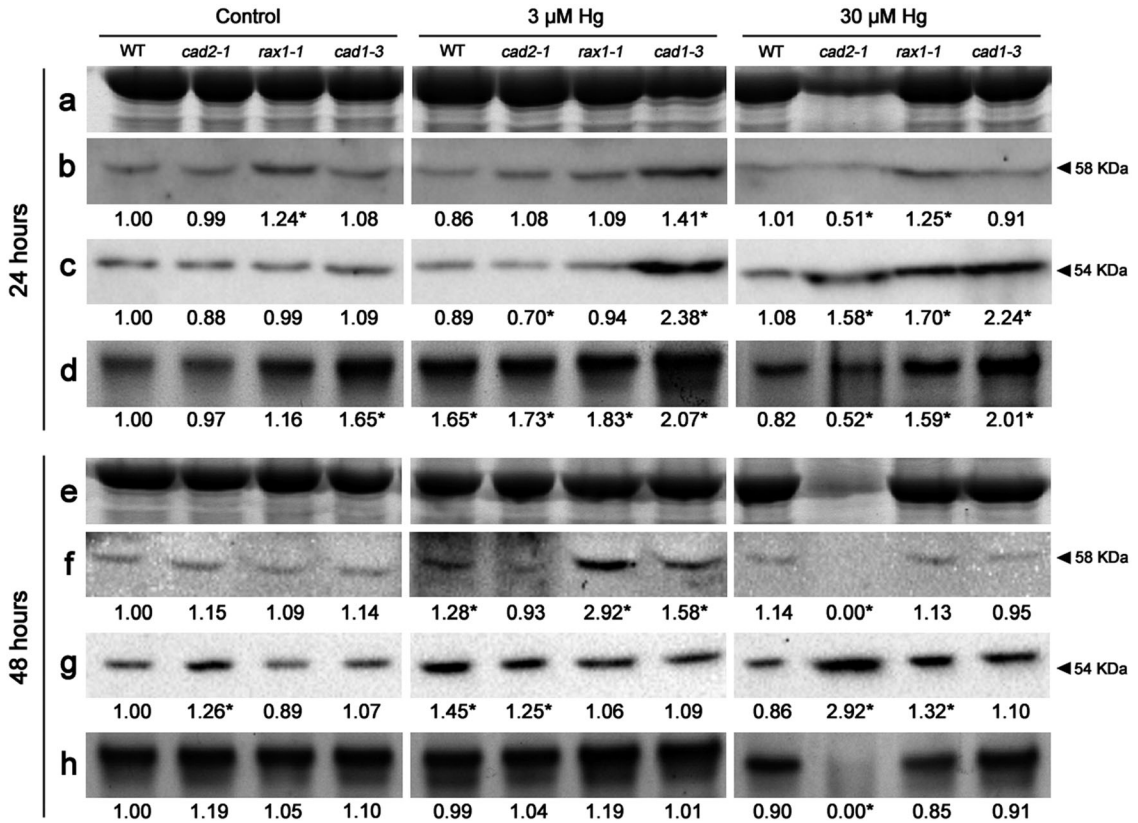

Fig. 6 Immunodetection of γECS (b and f), GR (c and g), and *in gel* GR activity (d and h) in 0, 3, and 30 μM Hg-infiltrated leaves of Col-0, *cad2-1*, *rax1-1* and *cad1-3 Arabidopsis thaliana* incubated for 24 and 48 h. Coomassie Blue (a and e) general staining of proteins to show the equivalent loading of samples. The numbers represent the relative fold-changes against the control, and asterisks mark changes greater than ±20%.

GSH catabolism occurs, leading to an increase in the GSH concentration, the catabolic activity of which is enhanced in Cd-treated seedlings.[35]

Recent work with high light stress in *Arabidopsis* showed the importance of the accumulation of ASA and GSH to protect against the overproduction of ROS.[36] The exposure of leaf disks to moderate doses of Cd or Hg (3 μM) for 24 h led to an increase in the GSH and GSSG concentrations that was significantly greater in non-γECS mutants. This increase was accompanied by a remarkable increase in the GSSG-to-total GSH ratio and, interestingly, an accumulation of ASA (Fig. 3A). However, at the highest doses of metals, these values dropped to those of the control samples, following a typical hormetic response. This pattern also occurred in leaf disks incubated for 48 h, where changes were less pronounced (Fig. 3B). A similar pattern was found in *Arabidopsis* hypocotyl cells treated with 50 μM Cd, where the GSH and PC concentrations increased after 24 h of incubation, but the GSH concentration decreased at longer exposure times.[37] Transient increases in the GSH and ASA concentrations were also reported in the root tips of *Poplar* hybrids under Cd stress (5 and 50 μM), which was accompanied by an increased GSSG-to-total GSH ratio and increased GR activity.[38] A transient accumulation of ASA and GSH occurred also under short-term Cd treatments in the roots of wheat seedlings and was accompanied by a significant increase in GR at the highest dose (40 μM).[39] In our case, the increase in ASA, GSH and GSSG concentrations under Cd and Hg was accompanied by higher GR activity and GR over-expression (Fig. 5 and 6). Therefore, it is feasible that under moderate metal stress conditions, the ASA–GSH antioxidant cycle is activated. However, this induction is repressed under acute stress conditions, attained at higher metal doses or prolonged exposures. In this sense, metal-sensitive genotypes such as *cad2-1* suffered stronger phytotoxic effects, as visualised by the severe inhibition in the activity of GR, an enzyme that is readily sensitive to Hg, under 30 μM Hg for 48 h (Fig. 6h).[26,40] Interestingly, GR was highly over-expressed in the *cad2-1* leaf disks, possibly following a compensatory mechanism to recover the GSH levels under metal stress.

The transient depletion of GSH with 30 μM Cd or Hg could be associated with the elevated production of PCs.[41] The importance of PC accumulation in Cd tolerance has been described in several plants;[42–45] biothiols also play a relevant role in the detoxification of Hg.[17,46] Metal–PC complexes are then sequestered in vacuoles by the action of ABCC tonoplast transporters.[47] In our experiments, both of the metals were clearly able to induce the synthesis of different PCs, Cd being a stronger inducer than Hg, as found by conventional HPLC and HPLC/ESI-MS(TOF), in accordance with previous studies performed in different plant species and under different growing conditions.[3,17,26,40]

As expected, the PC synthesis under Cd and Hg exposure depends completely on GSH metabolism, with remarkable differences between the two γECS allele mutants studied: *cad2-1* and *rax1-1* (Fig. 2, Table 1 and Table S1, ESI†). According to the literature, *cad2-1* has a limited capability to produce PCs due to its limited synthesis of GSH.[19] When exposed to 30 μM Cd for 48 h, *cad2-1* accumulated PC_2 and PC_3, while *rax1-1* also synthesised PC_4 according to the data of conventional HPLC (Fig. 2 and Table S1, ESI†). This result confirms previous observations where *cad2-1* accumulated a significantly lower concentration of PCs than did Col-0 when exposed to 30 μM Cd, while Hg failed to induce PCs or Hg–PC complexes.[17] However, less is known about the behaviour of *rax1-1* under metal stress, a mutant allele that is able to synthesise more GSH than can *cad2-1* and that is less sensitive to biotic and abiotic stresses.[20,48] These characteristics were confirmed by conventional HPLC and HPLC/ESI-MS(TOF), the data of which showed a lower number of PC ligands and lower values of their corresponding signal intensities in *cad2-1* than in *rax1-1*, an allele in which we could even detect PC_5 (Table 1). Therefore, *rax1-1* showed a response similar to that of Col-0 when treated with 30 μM Hg for 48 h, and we could even detect PC_6 in its leaf disks. These differences in PC accumulation between the γECS mutant alleles were also reflected in the Hg–PC complexes detected in the leaf disks that were exposed to Hg: *rax1-1* accumulated Hg–PC_2 and Hg–PC_3, although the intensity of these molecular ions was lower than that in Col-0 Hg-treated leaf disks, while Hg–PC complexes were not detected in *cad2-1* (compare Fig. 4A and B). Finally, the absence of Hg–PCs (for example in *cad2-1* and *cad1-3*) did not result in the accumulation of Hg–GSH complexes *in vivo*, in agreement with previous studies.[17,46]

In summary, we found that *rax1-1* exhibited a similar behaviour as that of Col-0 under Hg and Cd stress, despite the minor differences in the GSH concentration compared with *cad2-1*. Our results suggest that a decrease in the GSH concentration over a narrow threshold limits metal tolerance. The regulation of γECS is complex at the transcriptional and post-translational levels, as has been recently reported.[49,50] This complexity might explain the consistent over-expression of γECS in *rax1-1* leaf disks, reflecting possible modifications in the transcriptional pattern of S-metabolism genes. In this respect, Jobe *et al.*[31] found that altered levels of Cys or γECS in conjunction with the GSSG-to-total GSH ratio, as occurs in *cad2-1* and *rax1-1* mutants under metal stress, mediate the expression of *Sultr1;2*, a high-affinity sulphate transporter that is considered the first step in the sulphate assimilation process. Thus, the complete characterisation of the regulatory components of sulphur metabolism under metal stress, in particular in GSH-deficient mutants, should be a major task for future experiments to shed light on the mechanisms of metal tolerance in plants mediated by GSH.

Acknowledgements

This work was funded by the Ministry of Economy and Competitivity (Projects PROBIOMET AGL2010-15151 and AGL2010-16515), Junta Comunidades Castilla-La Mancha (FITOALMA2, POII10-007-6458), Comunidad de Madrid (EIADES consortium S2009/AMB-1478) and the Aragón Government (Group A03). We are extremely grateful to Prof. Phil Mullineaux (University of Essex, UK) and Prof. Chis Cobbett (University of Melbourne, Australia) for the donation of *rax1-1* and *cad1-3* mutant seeds, respectively.

References

1 European Commission, *Brussels*, **28**, 2005.
2 N. E. Selin, *Ann. Rev. Environ. Resour.*, 2009, **34**, 43–63.
3 R. Rellán-Álvarez, C. Ortega-Villasante, A. Álvarez-Fernández, F. F. Campo and L. E. Hernández, *Plant Soil*, 2006, **279**, 41–50.
4 F. Van Assche and H. Clijsters, *Plant, Cell Environ.*, 1990, **13**, 195–206.
5 C. Ortega-Villasante, L. E. Hernández, R. Rellán-Álvarez, F. F. Del Campo and R. O. Carpena-Ruiz, *New Phytol.*, 2007, **176**, 96–107.
6 R. Mittler, S. Vanderauwera, M. Gollery and F. Van Breusegem, *Trends Plant Sci.*, 2004, **9**, 490–498.
7 Y. Nakano and K. Asada, *Plant Cell Physiol.*, 1987, **28**, 131–140.
8 M. A. Hossain, P. Piyatida, J. A. Teixeira da Silva and M. Fujita, *J. Bot.*, 2012, DOI: 10.1155/2012/872875.
9 M. Jozefczak, T. Remans, J. Vangronsveld and A. Cuypers, *Int. J. Mol. Sci.*, 2012, **13**, 3145–3175.
10 G. Noctor and C. H. Foyer, *Annu. Rev. Plant Biol.*, 1998, **49**, 249–279.
11 G. Noctor, A. Mhamdi, S. Chaouch, Y. Han, J. Neukermans, B. Márquez-García, G. Queval and C. H. Foyer, *Plant, Cell Environ.*, 2012, **35**, 454–484.
12 H. Rennenberg, *Phytochemistry*, 1980, **21**, 2771–2781.
13 P. M. Mullineaux and T. Rausch, *Photosynth. Res.*, 2005, **86**, 459–474.
14 A. Wachter, S. Wolf, H. Steininger, J. Bogs and T. Rausch, *Plant J.*, 2005, **41**, 15–30.
15 C. H. Foyer and B. Halliwell, *Planta*, 1976, **133**, 21–25.
16 S. S. Gill, N. A. Anjum, M. Hasanuzzaman, R. Gill, D. K. Trivedi, I. Ahmad, E. Pereira and N. Tuteja, *Plant Physiol. Biochem.*, 2013, **70**, 204–212.
17 S. Carrasco-Gil, A. Álvarez-Fernández, J. Sobrino-Plata, R. Millán, R. O. Carpena-Ruiz, D. L. Leduc, J. C. Andrews, J. Abadía and L. E. Hernández, *Plant, Cell Environ.*, 2011, **34**, 778–791.
18 C. Cobbett and P. Goldsbrough, *Annu. Rev. Plant Biol.*, 2002, **53**, 159–182.
19 C. S. Cobbett, M. J. May, R. Howden and B. Rolls, *Plant J.*, 1998, **16**, 73–78.
20 L. Ball, G. Accotto, U. Bechtold, G. Creissen, D. Funck, A. Jimenez, B. Kular, N. Leyland, J. Mejia-Carranza and H. Reynolds, *Plant Cell*, 2004, **16**, 2448–2462.
21 R. Howden, P. B. Goldsbrough, C. R. Andersen and C. S. Cobbett, *Plant Physiol.*, 1995, **107**, 1059–1066.
22 C. Ortega-Villasante, R. Rellán-Álvarez, F. F. Del Campo, R. O. Carpena-Ruiz and L. E. Hernández, *J. Exp. Bot.*, 2005, **56**, 2239–2251.

23 W. E. Rauser, *Methods Enzymol.*, 1991, **205**, 319–333.
24 R. Rellán-Álvarez, L. E. Hernández, J. Abadía and A. Álvarez-Fernández, *Anal. Biochem.*, 2006, **356**, 254–264.
25 U. K. Laemmli, *Nature*, 1970, **227**, 680–685.
26 J. Sobrino-Plata, C. Ortega-Villasante, M. Laura Flores-Cáceres, C. Escobar, F. F. Del Campo and L. E. Hernández, *Chemosphere*, 2009, **77**, 946–954.
27 S. Carrasco-Gil, H. Siebner, D. L. LeDuc, S. M. Webb, R. Millán, J. C. Andrews and L. E. Hernández, *Environ. Sci. Technol.*, 2013, **47**, 3082–3090.
28 M. Válega, A. Lima, E. Figueira, E. Pereira, M. Pardal and A. Duarte, *Chemosphere*, 2009, **74**, 530–536.
29 E. Lozano-Rodriguez, L. E. Hernández, P. Bonay and R. Carpena-Ruiz, *J. Exp. Bot.*, 1997, **48**, 123–128.
30 V. Shanmugam, M. Tsednee and K. Yeh, *Plant J.*, 2012, **69**, 1006–1017.
31 T. O. Jobe, D. Y. Sung, G. Akmakjian, A. Pham, E. A. Komives, D. G. Mendoza-Cózatl and J. I. Schroeder, *Plant J.*, 2012, **70**, 783–795.
32 J. Davidian and S. Kopriva, *Mol. Plant*, 2010, **3**, 314–325.
33 S. Lee and S. Korban, *Planta*, 2002, **215**, 689–693.
34 R. Blum, K. C. Meyer, J. Wünschmann, K. J. Lendzian and E. Grill, *Plant Physiol.*, 2010, **153**, 159–169.
35 R. Blum, A. Beck, A. Korte, A. Stengel, T. Letzel, K. Lendzian and E. Grill, *Plant J.*, 2007, **49**, 740–749.
36 E. Heyneke, N. Luschin-Ebengreuth, I. Krajcer, V. Wolkinger, M. Müller and B. Zechmann, *BMC Plant Biol.*, 2013, **13**, 104.
37 R. De Michele, E. Vurro, C. Rigo, A. Costa, L. Elviri, M. Di Valentin, M. Careri, M. Zottini, L. S. di Toppi and F. L. Schiavo, *Plant Physiol.*, 2009, **150**, 217–228.
38 A. Schützendübel, P. Nikolova, C. Rudolf and A. Polle, *Plant Physiol. Biochem.*, 2002, **40**, 577–584.
39 A. Paradiso, R. Berardino, M. C. de Pinto, L. S. di Toppi, M. M. Storelli, F. Tommasi and L. De Gara, *Plant Cell Physiol.*, 2008, **49**, 362–374.
40 J. Sobrino-Plata, J. Herrero, S. Carrasco-Gil, A. Pérez-Sanz, C. Lobo, C. Escobar, R. Millán and L. E. Hernández, *RSC Adv.*, 2013, **3**, 4736–4744.
41 W. E. Rauser, *Plant Physiol.*, 1995, **109**, 1141–1149.
42 J. A. de Knecht, M. van Dillen, P. L. Koevoets, H. Schat, J. A. Verkleij and W. H. Ernst, *Plant Physiol.*, 1994, **104**, 255–261.
43 H. Schat, M. Llugany, R. VOOiJS, J. Hartley-Whitaker and P. M. Bleeker, *J. Exp. Bot.*, 2002, **53**, 2381–2392.
44 J. He, J. Qin, L. Long, Y. Ma, H. Li, K. Li, X. Jiang, T. Liu, A. Polle and Z. Liang, *Physiol. Plant.*, 2011, **143**, 50–63.
45 E. C. Bianucci, J. Sobrino-Plata, R. O. C. Ruíz, M. del Carmen Tordable, A. Fabra, L. Hernandez and S. Castro, *Metallomics*, 2012, **4**, 1119–1124.
46 L. Chen, L. Yang and Q. Wang, *Metallomics*, 2009, **1**, 101–106.
47 J. Park, W. Song, D. Ko, Y. Eom, T. H. Hansen, M. Schiller, T. G. Lee, E. Martinoia and Y. Lee, *Plant J.*, 2012, **69**, 278–288.
48 V. Parisy, B. Poinssot, L. Owsianowski, A. Buchala, J. Glazebrook and F. Mauch, *Plant J.*, 2007, **49**, 159–172.
49 M. Hothorn, A. Wachter, R. Gromes, T. Stuwe, T. Rausch and K. Scheffzek, *J. Biol. Chem.*, 2006, **281**, 27557–27565.
50 L. M. Hicks, R. E. Cahoon, E. R. Bonner, R. S. Rivard, J. Sheffield and J. M. Jez, *Plant Cell*, 2007, **19**, 2653–2661.

